

# Robustness and Directed Structures in Ecological Flow Networks

Taichi Haruna<sup>1</sup>

<sup>1</sup>Department of Earth & Planetary Sciences, Graduate School of Science, Kobe University,  
1-1, Rokkodaicho, Nada, Kobe 657-8501, Japan  
tharuna@penguin.kobe-u.ac.jp

## Abstract

Robustness of ecological flow networks under random failure of arcs is considered with respect to two different functionalities: coherence and circulation. In our previous work, we showed that each functionality is associated with a natural path notion: lateral path for the former and directed path for the latter. Robustness of a network is measured in terms of the size of the giant laterally connected arc component and that of the giant strongly connected component, respectively. We study how realistic structures of ecological flow networks affect the robustness with respect to each functionality. To quantify the impact of realistic network structures, two null models are considered for a given real ecological flow network: one is random networks with the same degree distribution and the other is those with the same average degree. Robustness of the null models is calculated by theoretically solving the size of giant components for the configuration model. We show that realistic network structures have positive effect on robustness for coherence, whereas they have negative effect on robustness for circulation.

## Introduction

Networks have been usually considered as undirected in the field of complex networks (Newman, 2003). However, many real-world networks are directed so that the direction of interaction is important for the functioning of the systems. Recently, it has been revealed that directed networks have richer structures such as directed assortativity (Foster et al., 2010) and flow hierarchy (Mones, 2013).

In our previous work, we proposed a new path notion involving directedness called lateral path that can be seen as the dual notion to the usual directed path (Haruna, 2011). Based on category theoretic formulation, we derived the lateral path as a natural path notion associated with the dynamic mode of biological networks: a network is a pattern constructed by gluing functions of entities constituting the network (Haruna, 2012). Thus, its functionality is coherence, whereas the functionality of the directed path is transport. We showed that there is a division of labor with respect to the two functionalities within a network for several types of biological networks: gene regulation, neuronal and ecological ones (Haruna, 2012). It was suggested that the two

complementary functionalities are realized in biological systems by making use of the two ways of tracing on a directed network, namely, lateral and directed.

In this paper, we address robustness of ecological flow networks with respect to the lateral path and directed path, respectively. Since the natural connectedness notion associated with the directed path is the strong connectedness, we consider robustness of the giant strongly connected component (GSCC) for the latter. For the former, robustness of the giant laterally connected component (GLCC) is of interest. Thus, we assess robustness of ecological flow networks in terms of two different functionalities, namely, coherence and circulation, both of which are important for the functioning of them (Ulanowicz, 1997).

Robustness of ecological networks is an intriguing issue in recent studies (Montoya et al., 2006; Bascompte, 2009). Initially, robustness of general complex networks has been argued qualitatively in terms of critical thresholds for the existence of the giant component (Albert et al., 2000; Cohen et al., 2001). For ecological networks, their robustness has been measured by the size of secondary extinctions (Solé and Montoya, 2001; Dunne et al., 2002). Here, we employ a recently proposed idea to measure robustness quantitatively (Schneider et al., 2011; Herrmann et al., 2011). As a first step, we consider only random failure of arcs. The size of giant components is measured by the number of arcs involved because laterally connected components are defined only on the set of arcs.

Here, we study the impact of realistic network structures on robustness with respect to the two functionalities. Two complementary measures of it are proposed by comparing the robustness of a given real network with that of the two null models: random networks with the same degree distribution and those with the same average degree. The robustness of the two null models is calculated by theoretically solving the percolation problem on the configuration model, random networks with an arbitrary degree distribution (Newman et al., 2001).

This paper is organized as follows. In Section 2, we develop a theory to calculate the size of GLCC and GSCC under

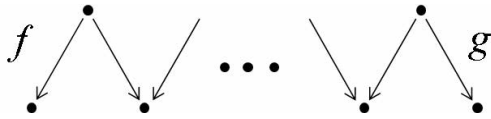


Figure 1: An example of lateral path.

random removal of arcs in the configuration model. In Section 3, we propose two measure for the impact of realistic structures on robustness of networks by using the theoretical result obtained in Section 2. In Section 4, the proposed measures are applied to 10 ecological flow networks. In Section 5, we discuss the results and indicate future directions.

### Random Removal of Arcs in the Configuration Model

In this section, we consider a percolation problem, random removal of arcs, in the configuration model with respect to the lateral connectedness and the strong connectedness.

A *lateral path* in a directed network is a path in the network such that the direction of arcs involved changes alternately (Haruna, 2012) (Fig. 1). Two arcs are called *laterally connected* if they are connected by a lateral path (Haruna, 2011). Lateral connectedness defines an equivalence relation on the set of arcs. Each equivalence class is called *laterally connected component*.

Since lateral connectedness is defined on the set of arcs, here we also consider strong connectedness for arcs. Two arcs are called *strongly connected* if there is a directed path from one arc to the other arc, and vice versa.

Let us consider a random directed network with degree distribution  $P(k_i, k_o)$ .  $P(k_i, k_o)$  is the fraction of nodes in the network with in-degree  $k_i$  and out-degree  $k_o$ . We make use of the generating function formalism (Callaway et al., 2000; Newman et al., 2001) to calculate the sizes of giant laterally or strongly connected components (in short, GLC-C or GSCC, respectively) after removing arcs uniformly at random with probability  $1 - \phi$ , where  $\phi$  is the occupation probability.

The generating function for  $P(k_i, k_o)$  is

$$G(x, y) = \sum_{k_i, k_o} P(k_i, k_o) x^{k_i} y^{k_o}. \quad (1)$$

The average degree  $z := \langle k_i \rangle = \langle k_o \rangle$  is given by

$$z = \frac{\partial G}{\partial x}(1, 1) = \frac{\partial G}{\partial y}(1, 1). \quad (2)$$

Let  $P_i(k_i) := \sum_{k_o} P(k_i, k_o)$  be the in-degree distribution and  $P_o(k_o) := \sum_{k_i} P(k_i, k_o)$  the out-degree distribution. Their generating functions are

$$F_0(x) := G(x, 1) \text{ and } H_0(y) := G(1, y), \quad (3)$$

respectively.

We introduce four excess degree distributions and corresponding generating functions that are necessary for the calculation in what follows.

First, let  $P_0(k)$  be the probability that the number of the other arcs arriving at the target node of a randomly chosen arc is  $k$  (Fig. 2 (a)). It is given by

$$P_0(k) := \frac{1}{z} \sum_{k_0} (k+1) P(k+1, k_0) \quad (4)$$

and its generating function is

$$F_{1,0}(x) := \sum_k P_0(k) x^k = \frac{1}{z} \frac{\partial G}{\partial x}(x, 1) = \frac{1}{z} \frac{\partial F_0}{\partial x}(x). \quad (5)$$

Second, let  $P_1(k)$  be the probability that the number of arcs arriving at the source node of a randomly chosen arc is  $k$  (Fig. 2 (b)). It is given by

$$P_1(k) := \frac{1}{z} \sum_{k_0} k_0 P(k, k_0) \quad (6)$$

and its generating function is

$$F_{1,1}(x) := \sum_k P_1(k) x^k = \frac{1}{z} \frac{\partial G}{\partial y}(x, 1). \quad (7)$$

Third, let  $Q_0(k)$  be the probability that the number of the other arcs leaving from the source node of a randomly chosen arc is  $k$  (Fig. 2 (c)). It is given by

$$Q_0(k) := \frac{1}{z} \sum_{k_i} (k+1) P(k_i, k+1) \quad (8)$$

and its generating function is

$$H_{1,0}(y) := \sum_k Q_0(k) y^k = \frac{1}{z} \frac{\partial G}{\partial y}(1, y) = \frac{1}{z} \frac{\partial H_0}{\partial y}(y). \quad (9)$$

Finally, let  $Q_1(k)$  be the probability that the number of arcs leaving from the target node of a randomly chosen arc is  $k$  (Fig. 2 (d)). It is given by

$$Q_1(k) := \frac{1}{z} \sum_{k_i} k_i P(k_i, k) \quad (10)$$

and its generating function is

$$H_{1,1}(y) := \sum_k Q_1(k) y^k = \frac{1}{z} \frac{\partial G}{\partial x}(1, y). \quad (11)$$

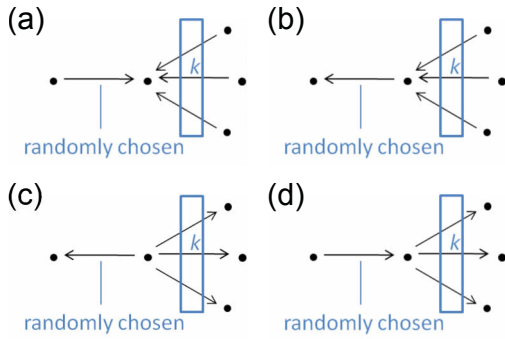


Figure 2: Four excess degree distributions. See the main text for details.

### Giant Laterally Connected Component

Let  $u$  be the average probability that an arc is not connected to the GLCC via a particular arc with the same target and  $v$  the average probability that an arc is not connected to the GLCC via a particular arc with the same source. Then, the average probability that an occupied arc does not belong to the GLCC is

$$\sum_{k,l} P_0(k) u^k Q_0(l) v^l = F_{1,0}(u) H_{1,0}(v). \quad (12)$$

Hence, the size of the GLCC is

$$L = \phi(1 - F_{1,0}(u) H_{1,0}(v)). \quad (13)$$

The values of  $u$  and  $v$  are calculated by the following set of equations:

$$\begin{cases} u = \sum_k Q_0(k)(1 - \phi + \phi v^k) = (1 - \phi) + \phi H_{1,0}(v) \\ v = \sum_k P_0(k)(1 - \phi + \phi u^k) = (1 - \phi) + \phi F_{1,0}(u). \end{cases} \quad (14)$$

The critical occupation probability  $\phi_{L,c}$  for the appearance of GLCC can be obtained from the linear stability analysis of the trivial solution  $(u, v) = (1, 1)$  of (14). It turns out to be

$$\phi_{L,c} = \frac{z}{\sqrt{(\langle k_i^2 \rangle - z)(\langle k_o^2 \rangle - z)}}. \quad (15)$$

### Giant Strongly Connected Component

The calculation of the size of the GSCC is similar to the node component case (Dorogovtsev et al., 2001; Schwartz et al., 2002). In (Serrano and De Los Rios, 2007), five notions of edge components are considered. For our purpose, consideration on the usual three components (in-, out- and strongly connected) as in the node component case are enough. However, these are implicit in the following calculation.

Let  $u$  be the average probability that an arc is not connected to the GSCC via a particular arc leaving from its target and  $v$  the average probability that an arc is not connected to

the GSCC via a particular arc arriving at its source. Then, the average probability that an occupied arc does belong to the GSCC is

$$\sum_{k,l} Q_1(k)(1 - u^k) P_1(l)(1 - v^l) = (1 - H_{1,1}(u))(1 - F_{1,1}(v)). \quad (16)$$

Hence, the size of the GSCC is

$$S = \phi(1 - H_{1,1}(u))(1 - F_{1,1}(v)). \quad (17)$$

The values of  $u$  and  $v$  are calculated by the following set of equations:

$$\begin{cases} u = \sum_k Q_1(k)(1 - \phi + \phi u^k) = (1 - \phi) + \phi H_{1,1}(u) \\ v = \sum_k P_1(k)(1 - \phi + \phi v^k) = (1 - \phi) + \phi F_{1,1}(v). \end{cases} \quad (18)$$

The critical occupation probability  $\phi_{S,c}$  for the appearance of GSCC is given by

$$\phi_{S,c} = \frac{z}{\langle k_i k_o \rangle}, \quad (19)$$

which is the same as in the node component case (Schwartz et al., 2002).

### Examples

We calculate the sizes of the GLCC and the GSCC as functions of the occupation probability  $\phi$  for three degree distributions: (a) Uncorrelated Poisson distribution (UPD)

$$P(k_i, k_o) = \frac{e^{-2\lambda} \lambda^{k_i+k_o}}{k_i! k_o!}, \quad (20)$$

(b) Uncorrelated exponential distribution (UED)

$$P(k_i, k_o) = \left(1 - e^{-1/\kappa}\right)^2 e^{-\frac{k_i+k_o}{\kappa}}, \quad (21)$$

and (c) Correlated Poisson distribution (CPD)

$$P(k_i, k_o) = \frac{e^{-\lambda} \lambda^{k_i}}{k_i!} \delta_{k_i, k_o}, \quad (22)$$

where  $\lambda, \kappa > 0$  are parameters and  $\delta_{k_i, k_o}$  is the Kronecker delta. The results are compared with numerical simulations in Fig. 3, which shows that the agreement between simulation and theory is well.

For critical occupation probabilities, we have  $\phi_{L,c} = \phi_{S,c} = 1/\lambda$  for UPD,  $\phi_{L,c} = (e^{1/\kappa} - 1)/2 < (e^{1/\kappa} - 1) = \phi_{S,c}$  for UED and  $\phi_{L,c} = 1/\lambda > 1/(\lambda + 1) = \phi_{S,c}$  for CPD. Thus, these examples also show that all possibilities  $\phi_{L,c} = \phi_{S,c}$ ,  $\phi_{L,c} > \phi_{S,c}$  and  $\phi_{L,c} < \phi_{S,c}$  actually occur.

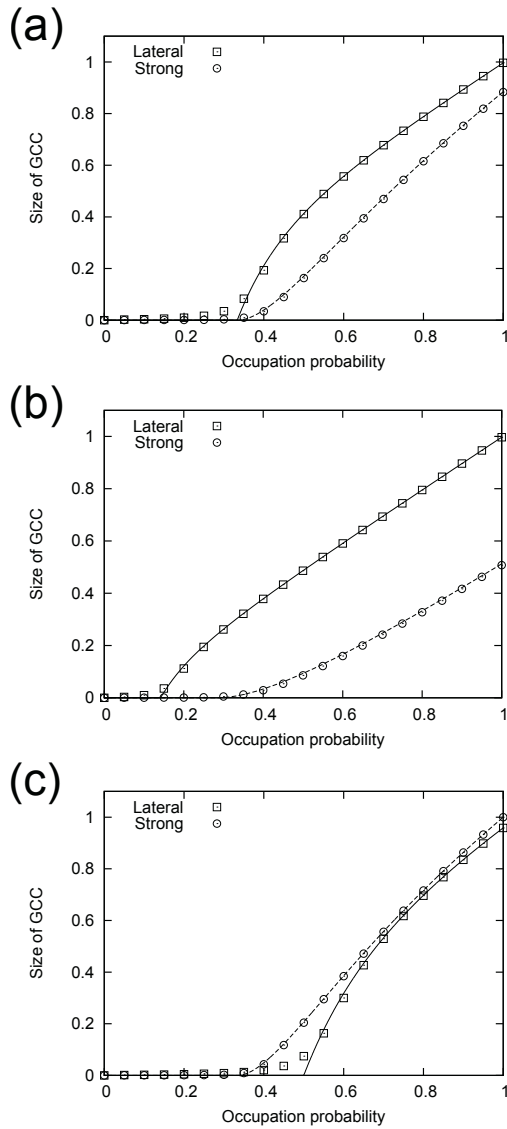


Figure 3:  $L(\phi)$  and  $S(\phi)$  for (a) the uncorrelated Poisson distribution with  $\lambda = 3$ , (b) the uncorrelated exponential distribution with  $\kappa = 4$  and (c) the correlated Poisson distribution with  $\lambda = 2$ . Lines are theoretically obtained. For (a) and (c), (14) and (18) are numerically solved. For (b), we obtain analytic expressions. Squares and circles are numerical simulations and averaged over 1000 different random removal sequences on different configuration model networks with the number of nodes 500 for (a) and (b), and 1000 for (c).

### Two Measures for Impact of Realistic Structures on Robustness

#### Robustness

Given a directed network, let  $L(\phi)$  be the size of the GLCC and  $S(\phi)$  the size of the GSCC for occupation probability  $\phi$ .

Motivated by the robustness measure proposed in (Schneider et al., 2011; Herrmann et al., 2011), we define the robustness of the GLCC and that of the GSCC by

$$R_L = \int_0^1 L(\phi)d\phi \text{ and } R_S = \int_0^1 S(\phi)d\phi, \quad (23)$$

respectively.

Our robustness measure is similar to link robustness in (Zeng and Liu, 2012), however, since we measure the size of a component by the number of arcs belonging to it, it is different from link robustness. In particular, since  $L(\phi)$  and  $S(\phi)$  cannot exceed the diagonal line, we have  $R_L, R_S \leq 0.5$ .

#### Gain

Given a directed network, we would like to consider how much its robustness (of the GLCC or the GSCC) is enhanced or degraded compared to a reference network. One measure is the ratio of the robustness of the given network to that of the reference network (Schneider et al., 2011). We call this measure *robustness gain*. If we denote the robustness of the given network by  $R_{given}$  and that of the reference network by  $R_{ref}$ , then the robustness gain is defined by

$$G_{given/ref} := R_{given}/R_{ref}. \quad (24)$$

We here consider three combinations of given-reference pairs: (given,ref)=(real, config), (given,ref)=(config, Poisson) and (given,ref)=(real,Poisson), where ‘real’ indicates a real-world network, ‘config’ the configuration model network with the same degree distribution and ‘Poisson’ the (uncorrelated) Poissonian network with the same average degree. The robustness gains for the three given-reference pairs are denoted by  $G_{r/c}$ ,  $G_{c/p}$  and  $G_{r/p}$ , respectively. Note that  $G_{r/p} = G_{r/c}G_{c/p}$ .

#### Complement Ratio

The other way to measure the effect of realistic structures on robustness is to evaluate the amount of unrealized robustness of the reference network (namely,  $0.5 - R$ ) utilized by the given network. We define the *robustness complement ratio* for the above three combinations of given-reference pairs by

$$C_{given/ref} := \frac{R_{given} - R_{ref}}{0.5 - R_{ref}}, \quad (25)$$

where  $(given, ref) = (r, c), (c, p)$  or  $(r, p)$ .

Both  $G_{given/ref}$  and  $C_{given/ref}$  are considered for the lateral connectedness and the strong connectedness in next section. We write  $G_{L,given/ref}$  and  $C_{L,given/ref}$  for the former and  $G_{S,given/ref}$  and  $C_{S,given/ref}$  for the latter.

### Ecological Flow Networks

In this section, we apply the indexes introduced in previous section to relatively large 10 networks (with the number of

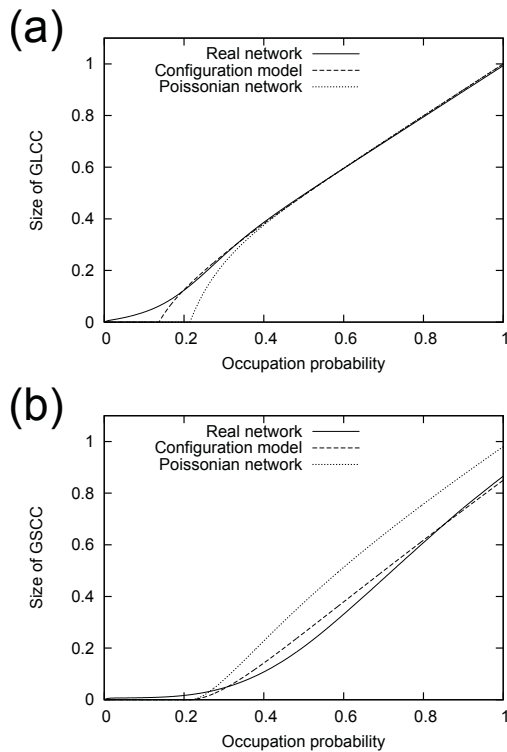


Figure 4: (a)  $L(\phi)$  and (b)  $S(\phi)$  for (vii) Middle Chesapeake Bay in Summer network (solid lines), those for the configuration model network with the same degree distribution (dashed lines) and those for the Poissonian network with the same average degree (dotted lines).

arcs  $> 100$ ) among 48 flow networks collected by R. Ulanowicz. Data are downloaded from <http://www.cbl.umces.edu/~ulan/ntwk/network.html>.

**Data**

Here, we list the 10 ecological flow networks we analyze. In the following,  $N$  is the number of nodes and  $A$  is the number of arcs included in the largest weakly connected component.  $z = \langle k_i \rangle = \langle k_o \rangle$  is the average degree. The number associated to each network is the web number in the original data source. In every network, each arc indicates the existence of carbon flow from its source to target. (i) Chesapeake Bay Mesohaline Network ( $N = 26, A = 122, z = 3.4$ , Web 34). (ii) Everglades Graminoids Wet Season ( $N = 66, A = 793, z = 12.0$ , Web 40). (iii) Final Narragansett Bay Model ( $N = 32, A = 158, z = 4.9$ , Web 42). (iv) Florida Bay Wet Season ( $N = 125, A = 1938, z = 15.5$ , Web 38). (v) Lake Michigan Control Network ( $N = 34, A = 172, z = 5.1$ , Web 47). (vi) Lower Chesapeake Bay in Summer ( $N = 29, A = 115, z = 4.0$ , Web 46). (vii) Middle Chesapeake Bay in Summer ( $N = 32, A = 149, z = 4.7$ , Web

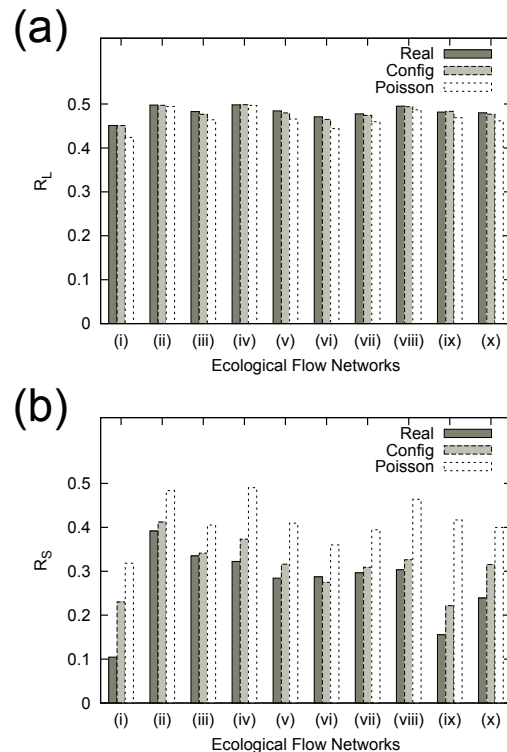


Figure 5: Robustness of (a) the GLCC and (b) the GSCC for the 10 ecological flow networks. Real: original networks, Config: the configuration model networks with the same degree distribution and Poisson: the Poissonian networks with the same average degree.

45). (viii) Mondego Estuary - Zostrea Site ( $N = 43, A = 348, z = 8.1$ , Web 41). (ix) St Marks River (Florida) Estuary ( $N = 51, A = 270, z = 5.3$ , Web 43). (x) Upper Chesapeake Bay in Summer ( $N = 33, A = 158, z = 4.8$ , Web 44).

**Results**

We plot  $L(\phi)$  (Fig. 4 (a)) and  $S(\phi)$  (Fig. 4 (b)) for (vii) Middle Chesapeake Bay in Summer network, the configuration model network with the same degree distribution and the Poissonian network with the same average degree, as a typical example.  $L(\phi)$  and  $S(\phi)$  for real ecological flow networks are calculated by averaging the size of the largest connected components over 1000 random removal sequences of arcs.

The robustness values for all 10 networks are shown in Fig. 5. One can see opposite tendency on how realistic structures influence robustness between the GLCC and the GSCC.  $R_L$  tends to increase as more realistic structures are imposed on one hand,  $R_S$  tends to decrease on the other hand. However, since  $R_L$  is close to 0.5 already for the Poissonian

Downloaded from <http://direct.mit.edu/saj/proceedings-pdf/ecal2013/25/179/1901397/978-0-262-31709-2-ch026.pdf> by guest on 23 April 2024

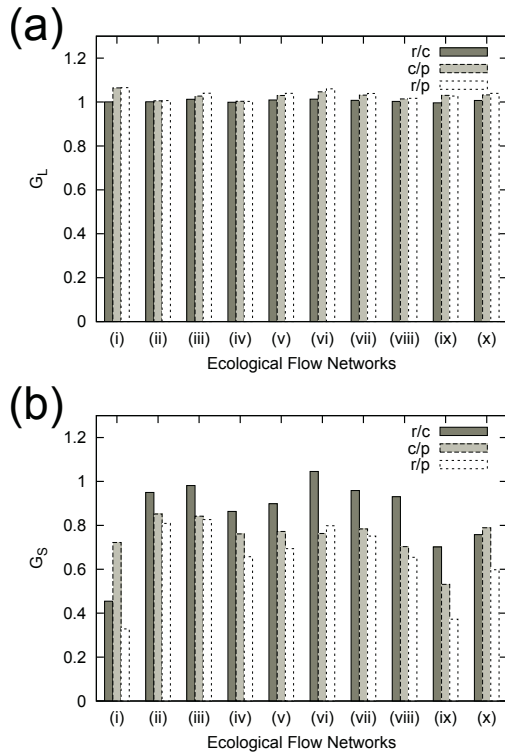


Figure 6: Robustness gain of the 10 ecological flow networks for (a) the GLCC and (b) the GSCC. Three given and reference network pairs are considered.  $r/c$ : (given,ref)=(real,config),  $c/p$ : (given,ref)=(config,Poisson) and  $r/p$ : (given,ref)=(real,Poisson). See the main text for details.

an network in most cases, the robustness gain for the GLCC is almost unity in all three given-reference pairs as seen in Fig. 6 (a). For  $R_S$ , one can see that the realistic degree distributions are the dominant factor for the degradation of robustness in most cases from Fig. 6 (b).

The tendency that realistic structures have positive impact on robustness of the GLCC can be captured more clearly by the robustness complement ratio as shown in Fig. 7. One can also see that the realistic degree distributions are the dominant factor to enhance the robustness of the GLCC in most cases.

### Discussions

Whether realistic structures of ecological networks have positive impact on their robustness or stability or not is controversial (Allesina and Tang, 2012). The answer to this question generally depends on the types of ecological interaction and dynamic processes of interest (Thébault and Fontaine, 2010; Allesina and Tang, 2012). In this paper, we focused on robustness of ecological flow networks under random failure of arcs with respect to the two different

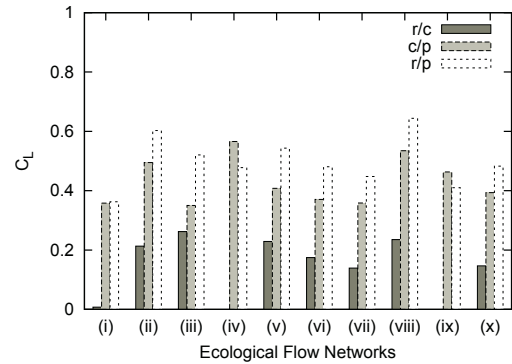


Figure 7: Robustness complement ratio of the 10 ecological flow networks for the GLCC. Three given-reference network pairs are considered.  $r/c$ : (given,ref)=(real,config),  $c/p$ : (given,ref)=(config,Poisson) and  $r/p$ : (given,ref)=(real,Poisson). Data that have negative values are omitted.  $C_S$  has negative values except one case (data not shown). See the main text for details.

functionalities, namely, coherence and circulation. The former is captured by the robustness of the GLCC and the latter by that of the GSCC. We found that they exhibit opposite tendency for constraints by the realistic network structures: the realistic network structures enhance the robustness of the GLCC on one hand, they degrade that of the GSCC on the other hand. In both case, it is suggested that the realistic degree distributions are one of the most important factors.

The former result seems to be consistent with the food-web stabilizing factor proposed in (Gross et al., 2009): “(i) species at high trophic levels feed on multiple prey species and (ii) species at intermediate trophic levels are fed upon by multiple predator species”, because such patterns in a network could contribute to make multiple lateral paths between arcs. Whereas, the latter result could provide a quantitative support for the ‘autocatalytic view’ on ecological flow networks proposed by R. Ulanowicz (Ulanowicz, 1997).

Our result in this paper suggests that complex networks can be both robust and fragile in a different sense from that in (Albert et al., 2000): under the same attack strategy, robust for one functionality and fragile for another functionality.

It is of interest whether the same tendency can be seen or not for the other various attack strategies (Holme and Kim, 2002) and for the other kinds of directed biological networks such as gene regulation and brain. Research results on these issues will be reported elsewhere near future.

### Acknowledgements

This work was partially supported by JST PRESTO program.

## References

- Albert, R., Jeong, H., and Barabási, A.-L. (2000). Error and attack tolerance of complex networks. *Nature*, 406:378–382.
- Allesina, S. and Tang, S. (2012). Stability criteria for complex ecosystems. *Nature*, 483:205–208.
- Bascompte, J. (2009). Disentangling the web of life. *Science*, 325:416–419.
- Callaway, D. S., Newman, M. E. J., Strogatz, S. H., and Watts, D. J. (2000). Network robustness and fragility: percolation on random graphs. *Phys. Rev. Lett.*, 85:5468–5471.
- Cohen, R., Erez, K., ben Avraham, D., and Havlin, S. (2001). Breakdown of the internet under intentional attack. *Phys. Rev. Lett.*, 86:3682–3685.
- Dorogovtsev, S. N., Mendes, J. F. F., and Samukhin, A. N. (2001). Giant strongly connected component of directed networks. *Phys. Rev. E*, 64:025101(R).
- Dunne, J. A., Williams, R. J., and Martinez, N. D. (2002). Network structure and biodiversity loss in food webs: robustness increases with connectance. *Ecology Letters*, 5:558–567.
- Foster, J. G., Foster, D. V., Grassberger, P., and Paczuski, M. (2010). Edge direction and the structure of networks. *Proc. Natl. Acad. Sci. USA*, 107:10815–10820.
- Gross, T., Rudolf, L., Levin, S. A., and Dieckmann, U. (2009). Generalized models reveal stabilizing factors in food webs. *Science*, 325:747–750.
- Haruna, T. (2011). Global structure of directed networks emerging from a category theoretical formulation of the idea “objects as processes, interactions as interfaces”. In Lenaerts, T., Giacobini, M., Bersini, H., Bourguine, P., Dorigo, M., and Doursat, R., editors, *Advances in Artificial Life, ECAL 2011, Proceedings of the Eleventh European Conference on the Synthesis and Simulation of Living Systems*, pages 310–317. MIT Press, Cambridge.
- Haruna, T. (2012). Theory of interface: category theory, directed networks and evolution of biological networks. arXiv:1210.6166.
- Herrmann, H. J., Schneider, C. M., Moreira, A. A., Andrade Jr, J. S., and Havlin, S. (2011). Onion-like network topology enhances robustness against malicious attacks. *J. Stat. Mech.*, P01027.
- Holme, P. and Kim, B. J. (2002). Attack vulnerability of complex networks. *Phys. Rev. E*, 65:056109.
- Mones, E. (2013). Hierarchy in directed random networks. *Phys. Rev. E*, 87:022817.
- Montoya, J. M., Pimm, S. L., and Solé, R. V. (2006). Ecological networks and their fragility. *Nature*, 442:259–264.
- Newman, M. E. J. (2003). The structure and function of complex networks. *SIAM Review*, 45:167–256.
- Newman, M. E. J., Strogatz, S. H., and Watts, D. J. (2001). Random graphs with arbitrary degree distributions and their applications. *Phys. Rev. E*, 64:026118.
- Schneider, C. M., Moreira, A. A., Andrade Jr, J. S., Havlin, S., and Herrmann, H. J. (2011). Mitigation of malicious attacks on networks. *Proc. Natl. Acad. Sci. USA*, 108:3838–3841.
- Schwartz, N., Cohen, R., ben Avraham, D., Barabási, A.-L., and Havlin, S. (2002). Percolation in directed scale-free networks. *Phys. Rev. E*, 66:015104(R).
- Serrano, M. A. and De Los Rios, P. (2007). Interfaces and the edge percolation map of random directed networks. *Phys. Rev. E*, 76:056121.
- Solé, R. V. and Montoya, J. M. (2001). Complexity and fragility in ecological networks. *Proc. R. Soc. Lond. B*, 268:2039–2045.
- Thébault, E. and Fontaine, C. (2010). Stability of ecological communities and the architecture of mutualistic and trophic networks. *Science*, 329:853–856.
- Ulanowicz, R. E. (1997). *Ecology, the Ascendent Perspective*. Columbia University Press, New York.
- Zeng, A. and Liu, W. (2012). Enhancing network robustness against malicious attacks. *Phys. Rev. E*, 85:066130.